Journal of Materials Chemistry A

Accepted Manuscript

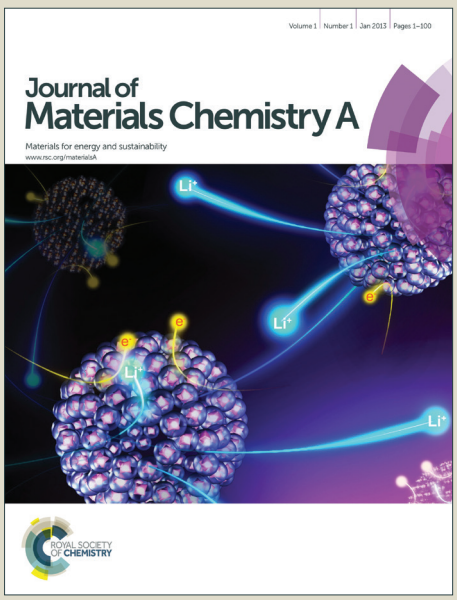

ROYAL SOCIETY OF CHEMISTRY

www.rsc.org/materialsA

Cite this: DOI: 10.1039/c0xx00000x

www.rsc.org/xxxxxx

COMMUNICATION

Sulfur Encapsulated in Porous Hollow CNTs@CNFs for High-Performance Lithium-Sulfur Batteries

Yuming Chen,[§⊥‡] Xiaoyan Li,[§‡] Kyu-Sung Park,[⊥] Jianhe Hong,[⊥] Jie Song,[⊥] Limin Zhou,[*§] Yiu-Wing Mai,[§,‖] Haitao Huang,[†] and John B. Goodenough[*⊥]

Received (in XXX, XXX) Xth XXXXXXXXX 200X, Accepted Xth XXXXXXXXX 200X

DOI: 10.1039/b000000x

Significant challenges for the commercialization of a lithium-sulfur battery include its rapid capacity fading and low power capability. Encapsulating the sulfur in pores of small volume of a porous carbon material alleviates this problem. We report a carbon-sulfur nanoarchitecture that encapsulates sulfur in porous hollow carbon-nanotubes@carbon-nanofibers (CNTs@CNFs) with a high Brunauer-Emmett-Teller (BET) specific surface area of 1400 m^2 g^{-1} and a total pore volume of 1.12 cm^3 g^{-1}. As a cathode, this material with 55 wt.% sulfur shows a high capacity of ~ 1313 mAh g^{-1} at 0.2 C, 1078 mAh g^{-1} at 0.5 C, 878 mAh g^{-1} at 1 C, 803 mAh g^{-1} at 1.5 C, 739 mAh g^{-1} at 2 C, and 572 mAh g^{-1} at 5 C, and maintains ~ 700 mAh g^{-1} at 1 C after 100 cycles and 430 mAh g^{-1} at 5 C after 200 cycles, which makes it a superior cathode material for a rechargeable Li-S battery.

The demand for electrical-energy storage for applications such as electric vehicles and large-scale grid energy storage drives research on safe lithium-ion batteries of higher energy density and lower cost.[1,2] Limiting factors are the low capacity of an insertion-compound cathode, especially if the lithium in the discharged cathode is lost to the passivation (SEI) layer on the anode on the initial charge. The introduction of an oxide/polymer membrane as a separator that blocks dendrites from a metallic-lithium anode makes possible consideration of a sulfur/lithium cell. If the low-cost, non-toxic sulfur cathode is discharged to Li_2S, the theoretical specific capacity of 1680 mAh g^{-1} and specific energy of 2600 wh kg^{-1} would provide a significant advance.[3-6] However, major challenges to a practical sulfur cathode include the solubility of the intermediate Li_2S_x ($2<x<4$) molecule in the electrolyte,[7,8] which must be blocked from reaching the anode and which creates a variable charge-dependent solute concentration in the cathode of a blocking, semipermeable polymer/oxide separator, thus creating an osmosis problem that is difficult to compensate by spectator solutes on the anode side of the separator. In addition, the poor electronic/ionic conductivity of sulfur limits the rate capability and efficient utilization of active material,[9-11] and a large volume expansion of *ca.*80% upon lithiation leads to pulverization of the active material with fast capacity decay.[12,13]

Attempts to address these problems with a sulfur cathode have included (i) fabrication of porous carbon/sulfur (C-S) nano composites for improving the electronic conductivity and trapping of the soluble polysulfides; [14-20] (ii) the use of alternative electrolytes or electrolyte modifiers; [21,22] and (iii) new binders to provide good bonding between the cathode composite and the current collector. [23,24] Among these methods, the most promising approach involves confining sulfur in a carbonaceous material such as carbon nanofibers (CNFs), carbon nanotubers (CNTs), graphene, or hollow carbon nanoparticles. [7,12,25,26] In order to improve the power capability and specific capacity from 1000 mAh g^{-1} at low rates as well as the potential for trapping of soluble species[7] sulfur has been encapsulated inside small volumes of a porous carbon matrix. [27,28]

Building on this promising strategy, we report a C-S nanoarchitecture that encapsulates amorphous sulfur in small pores in a hollow CNF that is enclosed by a conductive CNT (CNT@CNF) making electronic contact with the current collector. The hollow CNT@CNF morphology has a high specific Brunauer-Emmett-Teller (BET) surface area of ~ 1400 m^2 g^{-1} and a total pore volume of 1.1 cm^3 g^{-1}, As a cathode, this material with 55 wt.% sulfur shows a high capacity of ~ 1313 mAh g^{-1} at 0.2 C, 1078 mAh g^{-1} at 0.5 C, 878 mAh g^{-1} at 1 C, 803 mAh g^{-1} at 1.5 C, 739 mAh g^{-1} at 2 C, and 572 mAh g^{-1} at 5 C, and maintains ~ 700 mAh g^{-1} at 1 C after 100 cycles and 430 mAh g^{-1} at 5 C after 200 cycles. Such high performance can be ascribed to the unique nanoarchitecture, in which the synergistic advantages of C-S electrodes include improved electrical conductivity, and a better ability to accommodate effectively large volumetric expansion/shrinkage of sulfur during repeated lithiation/delithiation cycles, to trap the soluble polysulfides, and to shorten transport pathways for both Li ions and electrons.

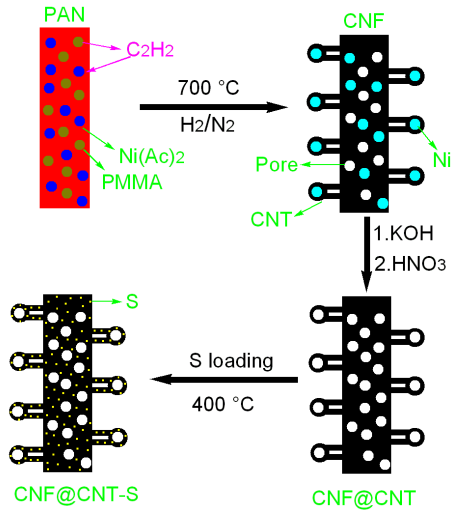

Figure 1. Schematic illustration of a novel C-S nanoarchitecture by encapsulating sulfur in porous hollow CNTs@CNFs.

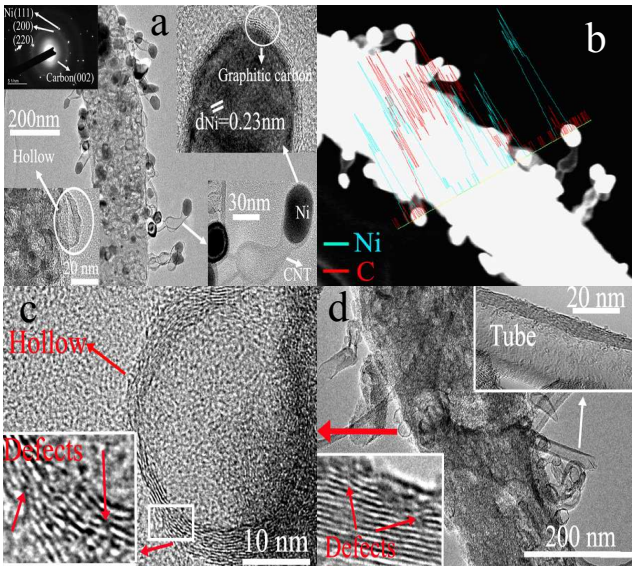

Figure 2. (a) SAED pattern, TEM and HRTEM images of CNTs@CNFs@Ni. (b) Dark-field TEM image and corresponding EDS line scanning of CNTs@CNFs@Ni. (c,d) TEM and HRTEM images of porous hollow CNTs@CNFs.

The porous hollow CNTs@CNFs-S is illustrated in Figure 1. Polyacrylonitrile (PAN) nanofibers have been shown to be an effective precursor for the fabrication of CNFs.[29,30] Sacrificial polymethylmethacrylate (PMMA) was introduced into PAN nanofibers to produce a porous structure in the resulting CNFs and C_2H_2 as a carbon resource for the growth of CNTs on the surface of the CNFs.[31-34] Nickel formed by the decomposition of nickel acetate ($Ni(Ac)_2$) acted as a typical transition metal for the graphitization of CNFs and the growth of CNTs.[29] To prepare porous hollow CNTs@CNFs, PAN/$Ni(Ac)_2$/PMMA composite nanofibers were first prepared by coaxial electrospining with a mixture of $Ni(Ac)_2$ and PAN as the outer fluid and PMMA as the inner fluid. PMMA could be distributed in the PAN matrix during the electrospinning process because of the use of the same DMF. The resultant composite nanofibers were pyrolyzed at 700 ºC in H_2(5 vol %)/N_2(95 vol %) for 6 h and then heated in vacuum for 6 h to produce CNTs@CNFs@Ni, followed by a combination of KOH activation and acid treatment to remove Ni particles, thus achieving porous hollow CNTs@CNFs. To obtain better impregnation of sulfur into the prepared carbon, we incorporated sulfur into porous hollow carbon by heating the S-C mixture at 400 °C for 24 h.[26]

Transmission electron microscopy (TEM) and high-resolution TEM (HRTEM, Figure 2a) images show that multiwalled CNTs grow on the surface of Ni@CNFs under the effect of a Ni catalyst formed by chemical vapor deposition. Many pores can be observed in Ni@CNFs owing to the decomposition of PMMA. The interplanar spacing of ~ 0.23 nm corresponds to the (010) plane of Ni nanoparticles encapsulated in graphitic carbon nanoparticles. The presence of crystalline Ni and carbon in the synthesized materials was further proved by the spot- and ring-like patterns in the selected-area electron diffraction (SAED, inset of Figure 2a). Figure 2b shows a dark-field TEM image and corresponding Energy-dispersive X-ray spectroscopy (EDS) line-scan profiles of the prepared materials (Figure S1†), further confirming that the composite materials consist of only Ni and carbon. After KOH activation and acid treatment, Ni nanoparticles are completely dissolved, yielding the pure porous hollow CNTs@CNFs. As shown in Figures 2c,d, it is clear that the diameter of the hollow nanospheres is about 20 nm and the inside and outside diameters of the CNTs are ~ 20 and 30 nm, respectively. The wall of the hollow structure contains many defects. The surface and pore size characterization of the porous hollow CNTs@CNFs was carried out by a nitrogen adsorption/desorption experiment. The hybrid materials show a high specific Brunauer-Emmett-Teller (BET) surface area of ~ 1400 m^2 g^{-1} and a total pore volume of 1.12 cm^3 g^{-1}. Type IV isotherms of the porous hollow CNTs@CNFs with distinct hysteresis loops, suggesting a characteristic of porous adsorption-desorption processes, is shown in Figure S2†.[35] Figure 3c displays the pore size distribution of the porous hollow CNTs@CNFs based on the Barrett-Joyner-Halenda (BJH) method. The porous hollow materials possess micropores and mesopores.

X-ray diffraction (XRD) patterns of the porous, hollow CNTs@CNFs in Figure 3a exhibits two peaks at ~ 24.95° and 44.75°, which are attributed to the (002) and (101) diffractions of carbon.[30] There is no diffraction peak related to crystalline sulfur in the CNTs@CNFs-S, indicating that sulfur in the porous hollow materials is amorphous. The C-S composites still show a relatively high BET surface area of ~ 80 m^2 g^{-1} with a total pore volume of ~ 0.2 cm^3 g^{-1}. Figure 3c displays only one peak of large space in CNTs@CNFs-S, showing that the sulfur is mainly encapsulated in the small-size pores. The X-ray photoelectron spectroscopy (XPS) S2p spectrum of the C-S composite in Figure S3† exhibits two peaks located at ~163.8 eV (S2p3/2) and 164.9 eV (S2p1/2) and the electron energy loss spectrum (EELS) of the C-S composite in Figure 3d shows a sulfur L-edge and carbon K-edge, further confirming the existence of sulfur in the porous hollow CNTs@CNFs.[36] Figure 3b shows the thermogravimetric analysis (TGA) of the C-S composite materials. A weight loss of

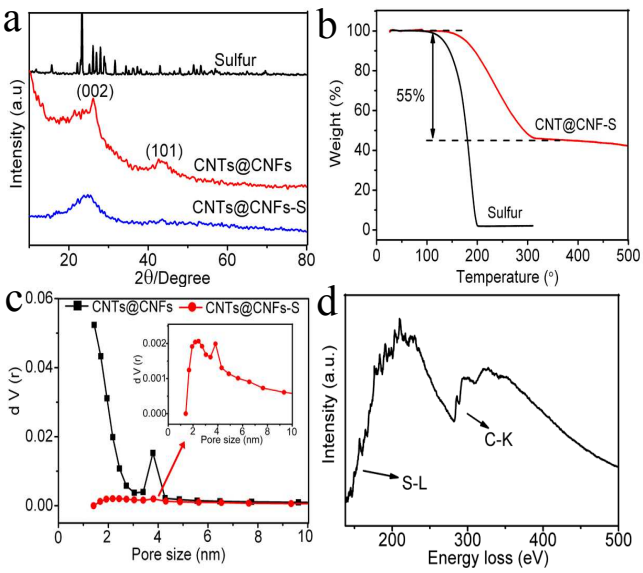

Figure 3. (a) XRD pattern of sulfur, porous hollow CNTs@CNFs, and porous hollow CNTs@CNFs-S. (b) TGA curves of sulfur and the porous hollow CNTs@CNFs-S. (c) Pore-size distribution of the porous hollow CNTs@CNFs and CNTs@CNFs-S. (d) EELS signal of sulfur L-edge and carbon K-edge of the porous hollow CNTs@CNFs-S.

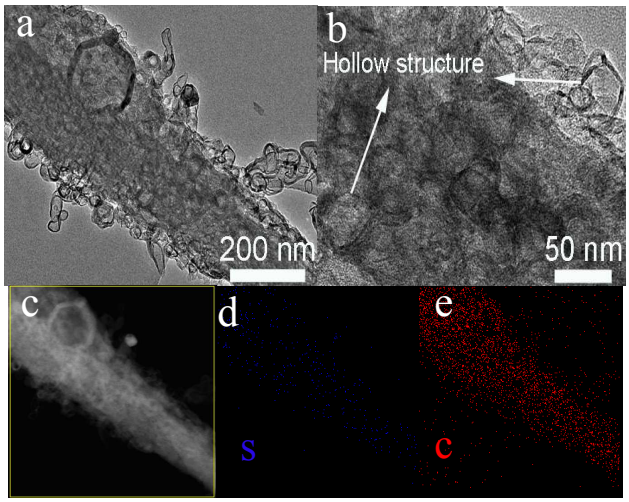

Figure 4 (a,b) TEM images of the porous hollow CNTs@CNFs-S. (c-e) Dark-field TEM image and corresponding EDS elemental mapping of the porous hollow CNTs@CNFs-S.

~55 % between 150 °C and 350 °C can be seen in the porous hollow CNTs@CNFs-S, corresponding to the evaporation of sulfur. Additionally, the thermal stability of the sulfur in the CNTs@CNFs-S is much better than that of pure sulfur particles, suggesting a strong interaction of carbon and sulfur.[26] Figures 4a-c show TEM and dark-field TEM images of the CNTs@CNFs-S. It is very clear that the prepared C-S composite materials still possess many hollow nanoparticles, indicating that the sulfur mainly exists in the small-size pores of the carbon matrix, which is consistent with the pore-size distribution result. Further evidence of sulfur in the hybrid carbon was provided by EDS. As shown in Figures 4d,e, the consistent signal in EDS mapping suggests uniform distribution of sulfur in the porous hollow CNTs@CNFs. The major reason for only a little sulfur material in the CNTs is because the CNTs are produced by *in situ* CVD and the porous hollow CNFs are from the calcination of polymer-based composite nanofibers. The density and diameter of defects in the CNFs are larger than those of the CNTs. Therefore, the sulfur preferably diffuses into CNFs.

Li-S cells were assembled to study the electrochemical performance of the CNTs@CNFs-S cathodes. The charge/discharge profiles of the CNTs@CNFs-S at different current rates in the voltage range of 1.5-3 V are shown in Figure 5a. Two plateaus at ~2.4 and 2.1 V are clearly observed during the discharge process; they can be ascribed to the formation of long-chain Li_2S_x ($4 \leq x \leq 8$) and short-chain Li_2S_2 and Li_2S, showing a typical behavior of a sulfur cathode.[9] In addition, the flat second plateau indicates a uniform deposition of Li_2S.[10] It was also observed that two plateaus are still clear when the current rate increases from 0.2 C to 5 C, showing good kinetics of the working electrode. At current densities of 0.2, 0.5, 1, 1.5, 2, and 5 C, the reversible capacities of the porous hollow CNTs@CNFs-S materials were ~ 1313, 1078, 878, 803, 739, and 572 mAh g^{-1}, respectively (Figure 5a,b). The cycling performance of the prepared hybrid electrode at 1 and 5 C is shown in Figure 5c. The reversible capacity still remains ~ 700 mAh g^{-1} at 1 C after 100 cycles and 430 mAh g^{-1} at 5 C after 200 cycles, which is much higher than that of CB-S (74 mAh g^{-1}), as shown in Figure S4†. The larger capacity loss at 1C as compared with 5C may be due to more side reactions caused by longer working time. In addition, the Coulombic efficiency of the porous hollow CNTs@CNFs-S nanomaterials was more than 97 % after the first few cycles, showing a good cycling stability at high current density. This performance is higher than the results reported for C-S composites such as hollow CNF-S, CNT-S, and graphene-S.[9,12,26] Figure 5d displays the cyclic voltammogram (CV) curves of the porous hollow CNTs@CNFs-S. Two main cathodic peaks at ~ 2.4 and 2 V seen in the prepared C-S composite materials is attributed to the S reduction to Li polysulfides, high-order Li polysulfides, and Li sulfides.[9] The observed oxidation reaction peak at ~2.4 V is ascribed to the conversion of Li_2S to Li polysulfide.[25] These results are similar to that of charge/discharge profiles. During the third to the ninth cycle, no obvious changes can be observed for both the cathodic and anodic peaks, suggesting the high electrochemical stability of the porous hollow CNTs@CNFs-S cathode. The high performance is the result of the unique structure of the synthesized materials with several favorable properties. First, the sulfur can be effectively encapsulated in the small-size pores and therefore the size of sulfur in CNTs@CNFs is small, which shortens transport pathways for both electrons and Li ions.[27,28] Second, the high surface area and hollow structure of the prepared materials can trap dissolved polysulfides and the hollow structure of the C-S composite can accommodate the large sulfur volumetric expansion during lithiation.[26] Third, the carbonaceous matrix with high electrical conductivity enables a good electrical connection to the active materials (The electrical conductivity of the C-S composite is ~0.8 S cm^{-1}).[13,17] Fourth, a strong interaction of carbon and sulphur can also enhance the cyclability.[37] In addition, further improvement could be achieved with an optimization of the characteristics of CNTs@CNFs (BET surface area, pore size distribution, and pore volume) and a Li^+-permeable solid-electrolyte interlayer, which can block the polysufide crossover.

Conclusions

In summary, we have successfully prepared a novel carbon-sulfur nanostructure by impregnating sulfur into porous hollow

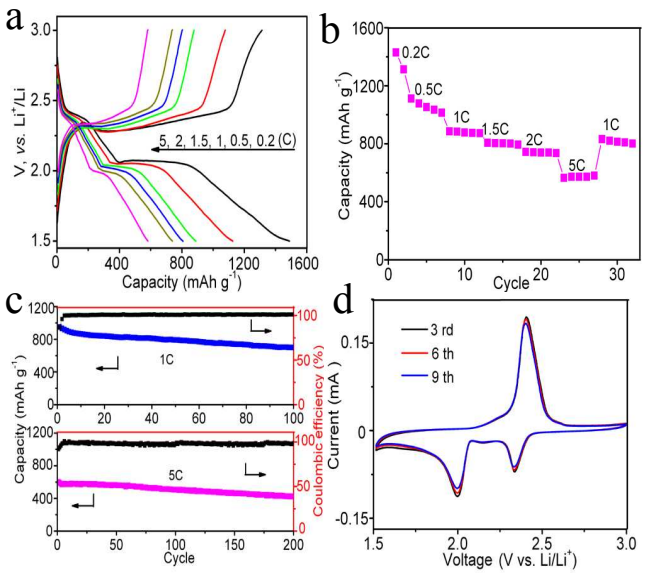

Figure 5. Electrochemical performance of porous hollow CNTs@CNFs-S for Li-S cell between 3 and 1.5 V *versus* Li^+/Li. (a) charge-discharge voltage

profiles, (b) rate capabilities at various current densities, (c) cycling stability at 1 and 5 C, and (d) CV curves.

CNTs@CNFs with a high specific surface area of 1400 m^2 g^{-1} and total pore volume of 1.12 cm^3 g^{-1}. Such unique advantages of C-S composite electrodes enable remarkable electrochemical performance with high capacity and good cycling life at high currents. These results show that such porous, hollow hybrid carbons are of great potential for high-power rechargeable Li-S batteries as next-generation energy storage systems.

Acknowledgements

The authors are grateful for the support received from the Research Grants Council of the Hong Kong Special Administration Region (grants: PolyU 5349/10E and PolyU 5312/12E) and the Hong Kong Polytechnic University (grants: G-YK47 and1-BD08). J.B.G thanks the Robert A. Welch Foundation of Houston, TX (Grant F-1066).

Notes and references

[§]Department of Mechanical Engineering and [†]Department of Applied Physics, The Hong Kong Polytechnic University, Hong Kong, China.

[‖]Centre for Advanced Materials Technology (CAMT), School of Aerospace, Mechanical and Mechatronics Engineering J07, The University of Sydney, NSW 2006, Australia.

[⊥]Texas Materials Institute and Materials Science and Engineering Program, The University of Texas at Austin, Austin, Texas 78712, United State.

Email:mmlmzhou@polyu.edu.hk; jgoodenough@mail.utexas.edu

‡These authors contributed equally.

† Electronic Supplementary Information (ESI) available: Synthetic details and additional experimental data. See DOI: 10.1039/b000000x/

1 P. G. Bruce, B. Scrosati and J.-M. Tarascon, *Angew. Chem., Int. Ed.*, 2008, **47**, 2930-2946.

2 R. Demir-Cakan, M. Morcrette, Gangulibabu, A. Gueguen, R. Dedryvere and J.-M. Tarascon, *Energy Environ. Sci.*, 2013, **6**, 176-182.

3 L. C. Yin, J. L. Wang, F. J. Lin, J. Yang and Y. N. Nuli, *Energy Environ. Sci.*, 2012, **5**, 6966-6972.

4 G. He, X. L. Ji and L. Nazar, *Energy Environ. Sci.*, 2011, **4**, 2878-2883.

5 Y. Yang, G. Y. Zheng and Y. Cui, *Energy Environ. Sci.*, 2013, **6**, 1552-1558.

6 J. B. Goodenough and K. S. Park, *J. Am. Chem. Soc.*, 2013, **135,** 1167-1176.

7 L. W. Ji, M. M. Rao, S. Aloni, L. Wang, E. J. Cairns and Y. G. Zhang, *Energy Environ. Sci.*, 2011, **4**, 5053-5059.

8 J. C. Guo, Y. H. Xu and C. S. Wang, *Nano Lett.*, 2011, **11**, 4288-4294.

9 A. Manthiram, Y. Z. Fu and Y. S. Su, *Acc. Chem. Res.*, 2013, **46**, 1125-1134.

10 B. L. Ellis, K. T. Lee and L. F. Nazar, *Chem. Mater.*, 2010, **22**, 691-714.

11 G. M. Zhou, D. W. Wang, F. Li, P. X. Hou, L. C. Yin, C. Liu, G. Q. Lu, I. R. Gentle and H. M. Cheng, *Energy Environ. Sci.*, 2012, **5**, 8901-8906.

12 Y. Yang, G. Y. Zheng and Y. Cui, *Chem. Soc. Rev.*, 2013, **42**, 3018-3032.

13 X. L. Ji and L. F. Nazar, *J. Mater. Chem.*, 2010, **20**, 9821-9826.

14 N. Jayaprakash, J. Shen, S. S. Moganty, A. Corona and L.A. Archer. *Angew.Chem. Int. Ed.,* 2011, **50**, 5904-5908.

15 C. D. Liang, N. J. Dudney and J. Y. Howe, *Chem. Mater.*, 2009, **21**, 4724-4730.

16 S. Jun, S. H. Joo, R. Ryoo, M. Kruk, M. Jaroniec, Z. Liu, T. Ohsuna and O. Terasaki, *J. Am. Chem. Soc.*, 2000, **122**, 10712-10713.

17 G. Zheng, Y. Yang, J. J. Cha, S. S. Hong and Y. Cui, *Nano Lett.*, 2011, **11**, 4462-4467.

18 L. Xiao, Y. Cao, J. Xiao, B. Schwenzer, M. H. Engelhard, L. V. Saraf, Z. Nie, G. J. Exarhos and J. Liu, *Adv. Mater.*, 2012, **24**, 1176-1181.

19 R. J. Chen, F. Wu, J. Z. Chen, S. X. Wu, L. Li, S. Chen and T. Zhao, *J. Phys. Chem. C*, 2011, **115**, 6057-6063.

20 X. Ji, S. Evers, R. Black and L. F. Nazar, *Nat. Commun.*, 2011, **2**, 325-311.

21 M. Sun, S. Zhang, T. Jiang, L. Zhang and J. Yu, *Electrochem. Commun.*, 2008, **10**, 1819-1822.

22 X. Yu, J. Xie, J. Yang and K. Wang, *J. Power Sources*, 2004, **132**, 181-186.

23 Y. Jung and S. Kim, *Electrochem. Commun.*, 2007, **9**, 249-254.

24 J. Sun, Y. Huang, W. Wang, Z. Yu, A. Wang and K. Yuan, *Electrochim. Acta*, 2008, **53**, 7084-7088.

25 X. Ji, K. T. Lee and L. F. Nazar, *Nat. Mater.*, 2009, **8**, 500-506.

26 C. F. Zhang, H. B. Wu, C. Z. Yuan, Z. P. Guo and X. W. David, *Angew. Chem., Int. Ed.*, 2012, **51**, 9592-9595.

27 J. Schuster, G. He, B. Mandlmeier, T. Yim, K. T. Lee, T. Bein and L. F. Nazar, *Angew. Chem., Int. Ed.*, 2012, **51**, 3591-3595.

28 S. Xin, L. Gu, N. H. Zhao, Y. X. Yin, L.J. Zhou, Y. G. Guo and L. J. Wan, *J. Am. Chem. Soc.*, **2012**, *134* , 18510-18513.

29 Y. M. Chen, Z. G. Lu, L. M. Zhou, Y. W. Mai and H. T. Huang, *Nanoscale,* 2012, **4**, 6800-6805.

30 Y. M. Chen, Z. G. Lu, L. M. Zhou, Y. W. Mai and H. T. Huang, *Energy Environ. Sci.,* 2012, **5**, 7898-7902.

31 L. E. Manring, *Macromolecules,* 1988, **21**, 528- 530.

32 S. J. Burge and C. F. H. Tipper, *Combust. Flame,* 1969, **13**, 495-505.

33 T. Kashiwagi, A. Inaba, J. E. Brown, K. Hatada, T. Kitayama and E. Masuda, *Macromolecules,* 1986, **19**, 2160-2168.

34 Y. Yu, L. Gu, C. B. Zhu, P. A. van Aken and J. Maier, *J. Am. Chem. Soc.,* 2009, **131**, 15984-15985.

35 Y. M. Chen, X. Y. Li, K. Park, J. Song, J. H. Hong, L. M. Zhou, Y. W. Mai, H. T. Huang and J. B. Goodenough, *J. Am. Chem. Soc.*, 2013, **135**, 16280-16283.

36 J. C. Guo, Z. C. Yang, S. Xu, Y. C. Yu , H. D. Abruña and L. A. Archer, *J. Am. Chem. Soc.*, 2013, **135**, 763-767.

37 L.W. Ji, M.M. Rao, H. M. Zheng, L. Zhang, Y. C. Li, W. H. Duan, J. H. Guo, E. J. Cairns and Y. G. Zhang, *J. Am. Chem. Soc.*, 2011, **133**, 18522-18525.

Graphical abstract

A novel architecture of carbon-sulfur nanoarchitecture by impregnating sulfur in porous hollow carbon-nanotubes@carbon-nanofibers (CNTs@CNFs) with a high Brunauer-Emmett-Teller (BET) specific surface area of 1400 m^2 g^{-1} and a total pore volume of 1.12 cm^3 g^{-1} shows a high capacity of 878 mAh g^{-1} at 1 C and 572 mAh g^{-1} at 5 C, and maintains ~ 700 mAh g^{-1} at 1 C and 520 mAh g^{-1} at 5 C after 100 cycles, which makes it a superior cathode material for a rechargeable Li-S battery.